A Pspice Model to Numerically Design Piezoelectric-Based Acoustic Power Transfer

Pierre Tacyniak, Martial Defoort, Skandar Basrour

A Pspice model to numerically design piezoelectric-based acoustic power transfer

Pierre Tacyniak
Univ. Grenoble Alpes, CNRS, Grenoble INP, TIMA*
38000 Grenoble, France
pierre.tacyniak@univ-grenoble-alpes.fr

Martial Defoort
Univ. Grenoble Alpes, CNRS, Grenoble INP, TIMA*
38000 Grenoble, France
martial.defoort@univ-grenoble-alpes.fr

Skandar Basrour
Univ. Grenoble Alpes, CNRS, Grenoble INP, TIMA*
38000 Grenoble, France
skandar.basrour@univ-grenoble-alpes.fr

***Abstract*—Acoustic power transfer (APT) has become a strategic stake with the increase of wireless smart devices located in electromagnetic proof environments. This is especially the case for medical implants where the transferred power has to go through human tissues, itself made of different layers (epidermis, dermis, muscle, bones), and through the metallic case of the medical implant. Each of these layers are mechanically coupled, making the optimization of the emitter and receiver of such system a complex task. To overcome this issue, we developed a procedure based on Pspice to accurately simulate APT between an emitter and a receiver, as it propagates through an intermediate layer. The procedure is based on Leach model which is the Pspice equivalent model of Mason electro-mechanical analogy. In this article, we propose a model which fits two 3-layer APT experiments, consisting in piezoelectric emitters and receivers with an intermediate layer of alternatively titanium and tungsten. The results provided by the simulations give a qualitative fitting of the APT and would enable to design, study and optimize n-layer APT systems for applications such as wireless medical implant recharging.**

Keywords—acoustic power transfer, piezoelectricity, Pspice.

I. Introduction

Wireless Power Transfer (WPT) has become an important subject of concern with the increase of electrical devices in our everyday life, wireless rechargers for phone for instance. Its application also interests the industry with the development of sensors set up in inaccessible places, inside pipes for example.

In the meantime, the medical field has also expressed a demand of miniaturization of medical implants [1]. However, the battery size can occupy up to 60% of the implant size [2] meaning that either the battery needs substantial improvements to overcome miniaturization, or the battery downsizing will imply a reduced autonomy of the implant. While the former is an active field of research, we focus this study on the latter. Since changing the battery would imply potentially harmful surgeries for the patient, recharging medical implants became one of the most sought solution, preferably with a wireless design for the patient's comfort, calling for new advances in WPT.

WPT relies on the principle of an emitter and a receiver separated by a passive material layer. WPT is commonly designed to work with two types of waves: electromagnetic or acoustic waves [3]. Electromagnetic-based WPT, usually using coils or antennas, is currently the most developed technic. However, electromagnetic waves have a low penetration depth in metallic structures, which are acting as a Faraday cage, and through water due to eddy current [3]. To overcome these obstacles, researches have been carried out on Acoustic Power Transfer (APT) which is immune to any form of electromagnetic shield.

APT is particularly well suited to supply medical implants, since the wave has to go through the human body, which is mainly composed of water, and through the structure packaging the implant, mostly metallic. Moreover, the safety requirements are more restrictive for electromagnetic waves than for acoustic waves: The Food and Drugs Administration (FDA) stated that the mean surface power density (I_{SPTA}) can go up to 100 mW.cm^{-2} for electromagnetic waves while acoustic waves can go up to 720 mW.cm^{-2} for general medical use cases [4]. For these reasons, our study focused on APT where its principle is visible on Fig. 1.

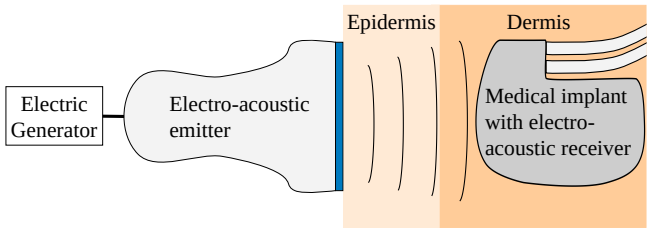

Fig. 1. Principle of Acoustic Power Transfer for medical implants.

APT can be designed with capacitive ultrasonic transducers, yet this solution needs to be powered with a continuous voltage to work [5]. This additional power consumption makes this design unsuitable for a receiver placed in a medical implant while the battery life of implants is critical. Thus, it is preferable to use piezoelectric transducers, crystals which can reversibly generate a current when deformed. Moreover, most of the ultrasonic probes used in the medical are designed with piezoelectric transducers [6].

II. System studied

As a first step of APT simulation for medical implant applications, we decided to consider as the intermediate layer solely the implant packaging, mostly designed with titanium. Our study was focused on a simplified system (Fig. 2) composed of two Ø20×0.8 mm SMD20T08F2500R [7] piezoceramics from STEMINC glued with non-conductive epoxy on each side of a square shaped 100×100×3 mm titanium plate, itself hold by a vise.

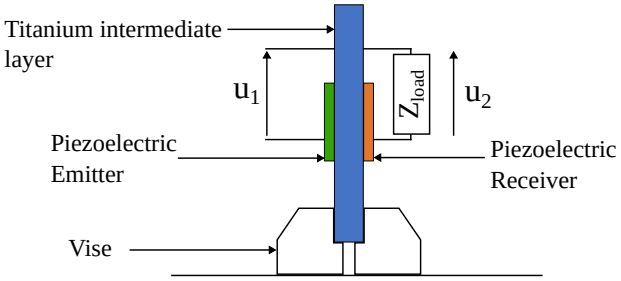

Fig. 2. 3-layer acoustic power transfer experimental package.

One transducer, the emitter, is powered by an Agilent 33500B generator and the other transducer, considered as the receiver, has a 75 Ω optimal load resistance put in parallel of it [8].

Following FDA requirements which limits the frequency of the ultrasounds from 1 MHz to 20 MHz, and because the higher the working frequency is, the higher the losses are in WPT [9], we decided to restrain our study from 1 MHz to 5 MHz. Therefore, the generator performs a frequency sweep of 841 points between these frequencies, providing a precision of 5 kHz, and we set the voltage generator to 1 Volt.

Measurement are carried out on the voltage at the terminal of each transducer by a Picoscope 3404D. The input voltage U_1 of the APT stands for the voltage of the emitter while the output voltage U_2 stands for the voltage of the receiver. For each frequency, the voltage is averaged over 5000 periods to reduce possible interferences. As transducers are mechanical systems, meaning long transient time, each frequency change is followed by 100 ms of waiting time before measurement.

III. Theory

The piezoelectric transducer disks can have different vibrational modes. We decided to focus our work on the thickness modes of the transducers as they were designed for these modes and as the acoustic waves propagates along these modes.

A. Mason model

To model the experiment, an electromechanical analogy is possible through Mason model [10]. This 1D simplified theory models the mechanical behavior of a layer with a quadrupole and a piezoelectric layer as a hexapole which consists in the previous quadrupole with the addition of an electrical part modelling the electromechanical conversion.

The model of a layer of material takes into account three different properties:

Geometric properties:

- The thickness t (m).
- The normal area A (m^2).

Material properties:

- The density ρ ($kg.m^{-3}$).
- The elastic constant c_{33} (Pa).
- The mechanical quality factor Q_m.

Piezoelectric properties:

- The piezoelectric constant h_{33} ($V.m^{-1}$).
- The dielectric permittivity ε_{33} ($F.m^{-1}$).
- The dielectric loss factor tan δ.
- The piezoelectric conversion loss factor tan θ.

It is important to note that the generator, the cables or the electrical circuit of the implant can modify the electrical behavior of APT, making difficult to fit theory to experiment. As Pspice library is composed of pre-established electrical component models, we decided to simulate this model on this software (Fig. 3). Moreover, this library also facilitates the design and integration of the APT to a complete wireless rechargeable implant system.

B. Leach model

Pspice piezoelectric model have been designed by Leach and completed by other researches [11], [12]. Here, the mechanical part of a layer is replaced by a transmission line and the piezoelectric part by Laplace functions. Even if such

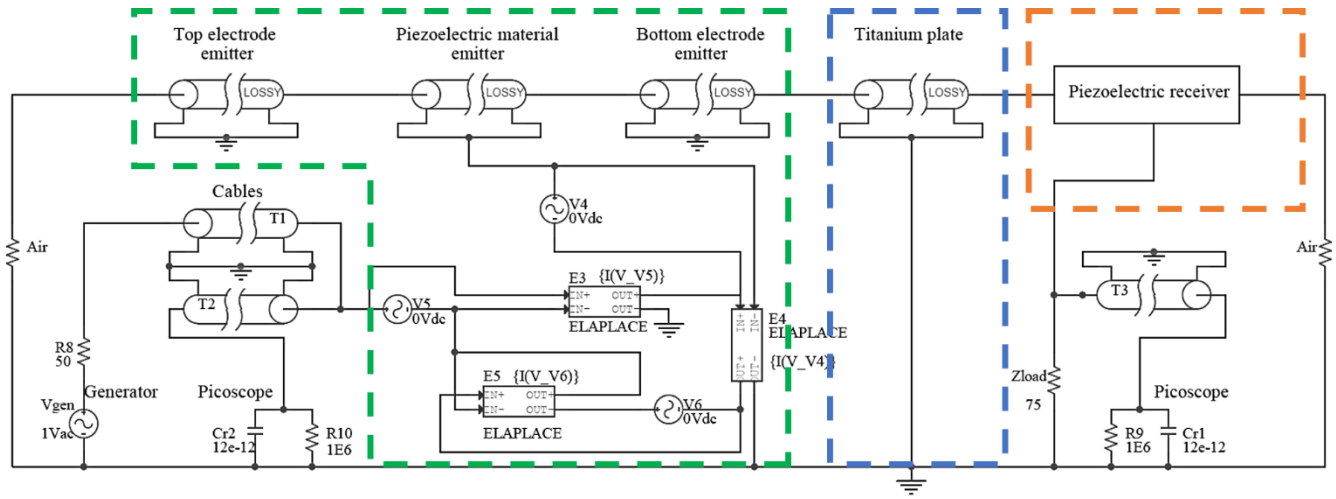

Fig. 3. Pspice model for simulating acoustic power transfer of a 3-layer system. Each layer of Fig. 2 is squared with the corresponding color. The three lossy transmission lines of the emitter correspond to the electrodes and the piezoelectric material. T1, T2, T3 are the cables. R10, R9 and Cr1, Cr2 are the inputs of the Picoscope. Vgen and R8 corresponds to the Thevenin equivalent model of the generator.

systems have already been modeled, none of them have proposed a predictive model of APT.

C. APT model

In our case, the Pspice model is visible on Fig. 3. Each layer of Fig. 2 is squared with the corresponding color on Fig. 3 for better understanding. Due to the sensitivity of our experimental system, we modelled the full electrical circuit which includes the impedance R8 of the generator (Thevenin model), the cables with transmission lines T1, T2 and T3 and the Picoscope's inputs with R10/Cr2 and R9/Cr1.

A transducer is composed of three mechanical layers: two for the electrodes and one for the piezoelectric material. Although, the thickness of the electrodes is negligible compared to the material's one, neglecting them has a significant impact on the fitting results and on the values of the parameters. For instance, not taking into account the electrodes of the emitter would make the fitting algorithm estimate a thinner transducer (0.80 mm) than in reality (0.87 mm). The material chosen for the electrodes were nickel as they are the most common material used.

D. Results

1) Titanium plate

The experimental results show that the frequency responses of the transducers have three major resonance frequencies between 1 and 3 MHz as visible on Fig. 4 and Fig. 5. These resonances characterize different modes of the system and not only the resonances of the transducers. Experimentally, a mode can either be a thickness mode, a radial mode, a flexural mode or a mix of multiple modes. Furthermore, one mode can characterize a single layer of the system but also multiple layers in the meantime, a coupled mode. For instance, a resonance can be a mode of one of the transducers or a mode of the titanium plate but it can also be a mode of both layers in the meantime. For the purpose of medical implants applications, other layers such as skin, soft tissues or bones will have to be taken into account. Since each person has a different anatomy, modes resulting from the coupling between different layers are more subject to change from one person to another. The coupling between the layers and its impact on APT will be discussed elsewhere, but for the scope of this study we decided to focus on the mode arising from the intermediate metallic layer only - in this case, the modes located between 2 and 3 MHz - which should ease future implementation.

In order to fit our model, we used Pspice Optimizer with the Least-Square method. For the fit, all the parameters values were measured or estimated with material database or given by the manufacturer's datasheets. Except for the quality factors, we added a confidence interval of 10% around the previously mentioned values letting the Optimizer test enough but realistic input values. The results provided by the simulation are visible on Fig. 4 and the parameters of the fit are presented in Table 1.

All the geometric dimensions were measured with a caliper except for the electrodes which were not measureable as they were already assembled with the piezoelectric material. The mass of the titanium plate was also measured.

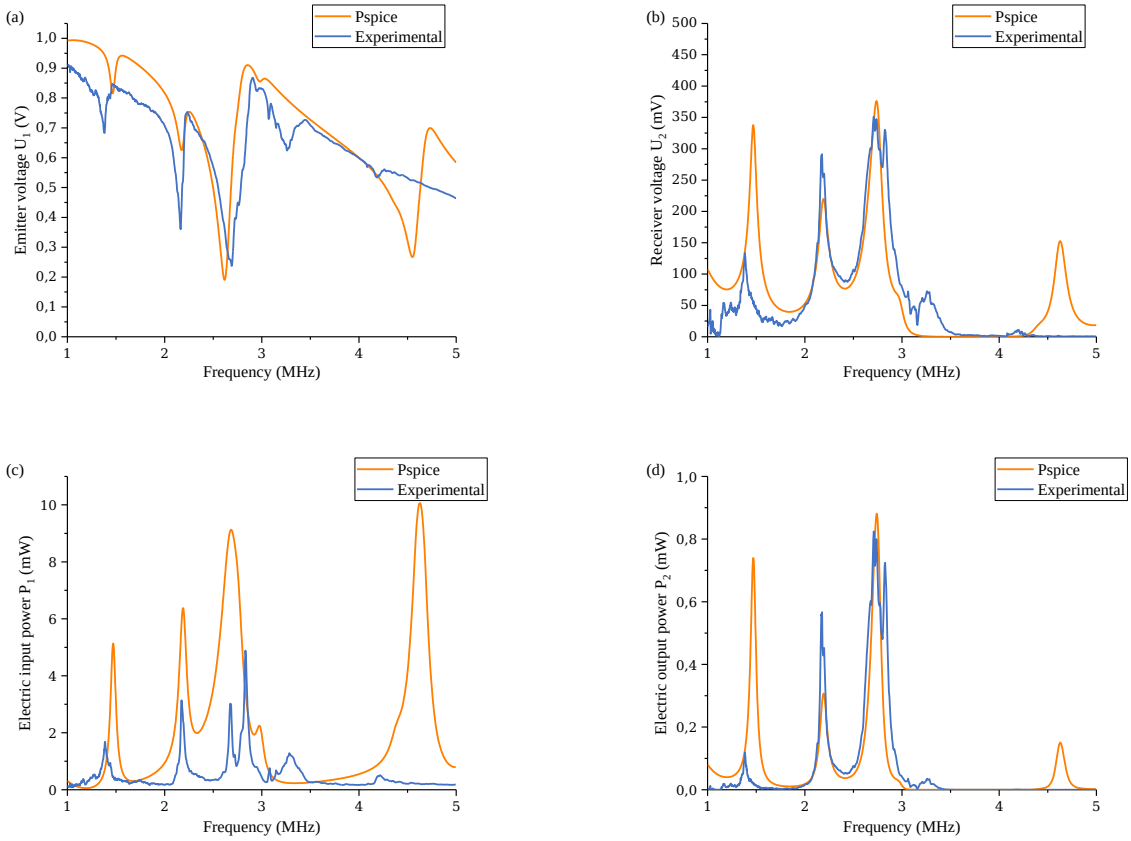

Fig. 4. Pspice experimental fit results for a titanium intermediate layer. U_1 (a), U_2 (b) corresponds to the input and the output voltages and P_1 (c), P_2 (d) to the input and the output powers. The Pspice model was fit on U_1 and U_2 and on the resonances between 2 and 3 MHz.

TABLE 1. FITTING PARAMETERS COMPARED TO MANUFACTURER'S DATA FOR THE TITANIUM APT. THE PARAMETERS ESTIMATED VIA EXTERNAL DATA ARE INDICATED WITH AN ASTERISK. THE GEOMETRIC DIMENSIONS WERE MEASURED WITH A CALLIPER WITH EXCEPTION FOR THE ELECTRODES.

Parameters	**Top electrode emitter**	**Piezoelectric material emitter**			**Bottom electrode emitter**	**Titanium plate***			**Bottom electrode receiver**	**Piezoelectric material receiver**			**Top electrode receiver**
	Fitting	***Data***	***Fitting***	***Δ (%)***	***Fitting***	***Data***	***Fitting***	***Δ (%)***	***Fitting***	***Data***	***Fitting***	***Δ (%)***	***Fitting***
t (mm)	0.015	0.87	0.80	5	0.013	3.1	3.3	6.5	0.018	0.86	0.80	3.1	0.015
A (mm^2)	314	314	314	0	314	1.10^4	1.10^4	0.1	314	314	314	0	314
ρ ($g.cm^{-3}$)	8.9	7.9	7.9	0	8.9	4.44	4.44	0	8.9	7.9	7.9	0	8.9
c_{33} (GPa)	208	73*	73	0	208	116	116	0	208	73*	73	0	208
Q_m (1)	100	1800	50	97	100		30		100	1800	50	97	100
h_{33} ($\times 10^9$ $V.m^{-1}$)		1-4*	2.5							1-4*	2.5		
ε_{33} ($F.m^{-1}$)		1400	1400	0						1400	1400	0	
tan δ (%)		0.4	0.42	5						0.4	0.43	7.5	
tan θ (%)*			4								4		

The mechanical properties of Titanium and Nickel were provided by the database of Matweb.com [13].

The piezoelectric transducers data were provided by STEMINC [14] with exception for h_{33} and c_{33} which were estimated after bibliographic study.

In Table 1, the difference Δ between the fit and the measured thicknesses of the piezoelectric material takes into account the thicknesses of the electrodes. Without taking into account the electrodes, the difference would be 8% and 7% for the emitter and the receiver respectively.

The fit Pspice model provides a qualitative result with a global error between the experimental curve and the model of 13% for the input voltage U_1 and 60% for the output voltage U_2 and P_2, this error falls to 20% between 2 and 3 MHz. The input power P_1 has a difference of 60%. In the meantime, the model provides an accurate prediction of the frequency location of the modes for the voltages and the powers.

All the parameters values are located into the expected confidence interval except for the quality factor with a difference of 97% in comparison to the datasheet. After measurement of the bandwidth of the resonance at 2.7 MHz, the quality factor measured seems to correspond to the quality factor provided by Pspice. It is likely that the value provided in the datasheet either does not apply to the modes we are studying, or the coupling with the intermediate layer degrades the overall quality factor.

Currently, the model only takes into account thickness modes which can explain the difficulty to fit the amplitude of the resonance located at 1.37 MHz and at 4.18 MHz. In fact, STEMINC provides the frequency constants of its transducers which enabled us to calculate the theoretical location of each modes:

$$f_r^t = nN_t/t \quad (1)$$

$$f_r^R = nN_p/d \quad (2)$$

where f_r^t is the thickness resonance frequency of a transducer, f_r^R is the radial resonance frequency of a transducer, n is a natural number, N_t and N_p the frequency constants, d and t the diameter and the thickness of the transducer respectively.

The results of (1) shows that the first thickness mode of the transducers is located at 2.6 MHz corresponding to the third resonance visible on Fig. 4 (b). In the meantime, the other resonances seem to correspond to the theoretical frequency location of radial modes calculated with (2). Including the radial modes of piezoelectric transducers in Pspice has already been done in the literature and seems to have a non-negligible role on the simulation results [15].

Furthermore, the titanium plate also has its modes which may occur during the measurement. The natural frequencies of a plate were estimated with Finite Element Method. The results provided showed that the 1.37 MHz and 4.16 MHz also seem to correspond to a combination of multiple modes of the plate. Thus, we assume that the coupling of the radial modes of the transducers with the addition of the plate modes could attenuate the APT and provide these experimental results.

We also decided not to model the glue located between the transducers and the plate as it could be difficult to measure its actual thickness or continuity. Moreover, simulating the glue would make the model more complex with 2×5 parameters to fit (cf. III.A). Consequently, we can observe that the thickness of the plate is fit to a slightly higher thickness than expected as it presents an additional thickness of passive material.

Finally, the glue is mostly an acoustic binder between the transducers and the titanium. In fact, without glue, the air would create an impedance mismatch and would consistently reduce the efficiency of power transfer.

2) Tungsten plate

The acoustic impedance characterizes the ability of a material to propagate an acoustic wave. When an acoustic wave reaches an interface between two layers, the wave can behave differently depending on the acoustic impedances difference between the layers. If the acoustic impedances of both layers are close, then the wave crosses the layers' interface and goes through the second layer. However, if the two layers have different impedances then there is an impedance mismatch, thereby the wave is partially

reflected on the interface and goes back into the first layer. The unit of acoustic impedance is the Rayl (Pa.s.m^{-1}) [16].

In the case of titanium, the impedance mismatch is low as titanium and piezoelectric materials have close acoustic impedances (around 20-25 MRayls). However, for medical implants, the APT will go through the skin, the muscle (1.7 MRayls) or the bones (from 2.5 to 6.7 MRayls) creating important impedance mismatches and thus modifying the behavior of the APT.

Therefore, we decided to test our Pspice model with an important acoustic impedance mismatch by changing the intermediate layer with a 50×50×3.2 mm tungsten plate (90 MRayls). We also changed the transducers to Ø15×0.5 mm NCE51 piezoceramics from NOLIAC [17], enabling to test the adaptability of our model. The results provided are visible on Fig. 5 and the fitting parameters are

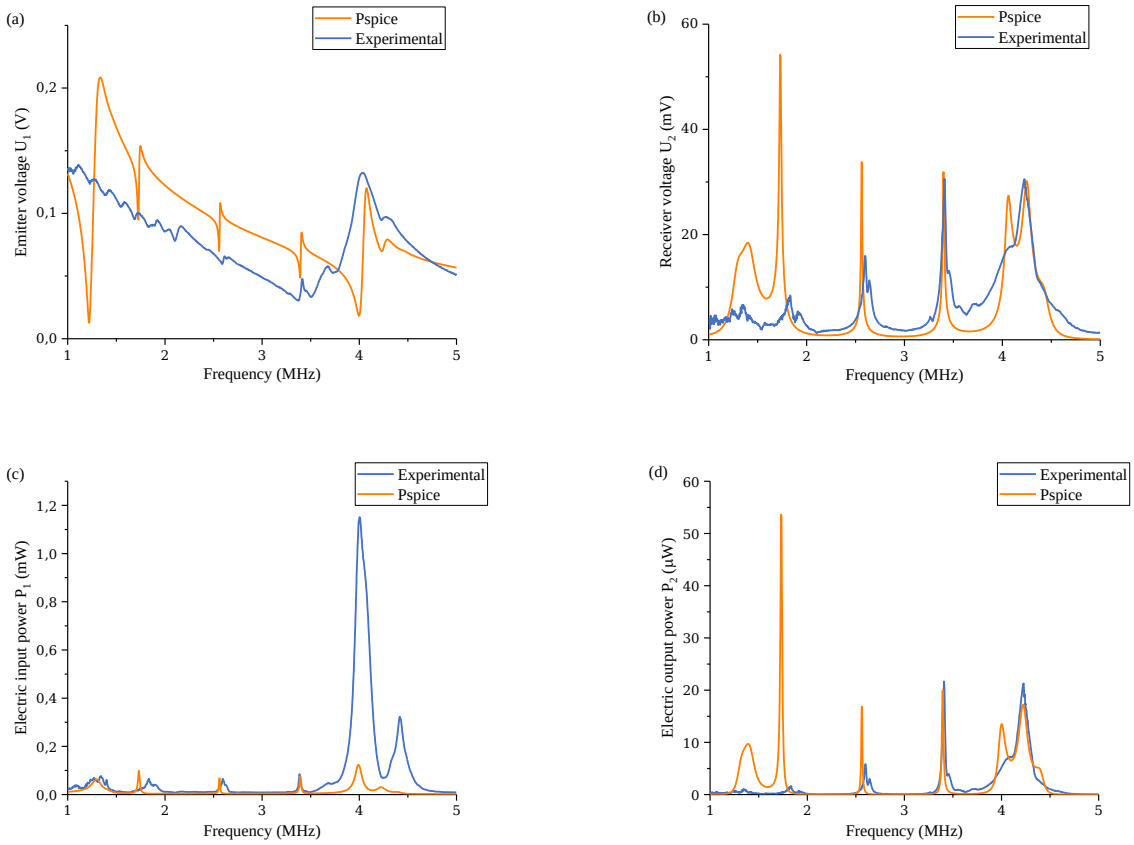

Fig. 5. Pspice experimental fit results for a titanium intermediate layer. U_1 (a), U_2 (b) corresponds to the input and the output voltages and P_1 (c), P_2 (d) to the input and the output powers. The Pspice model was fit on U_1 and U_2 and on the resonances located between 2 and 3.5 MHz.

TABLE 2. FITTING PARAMETERS COMPARED TO MANUFACTURER'S DATA FOR THE TITANIUM APT. THE PARAMETERS ESTIMATED VIA EXTERNAL DATA ARE INDICATED WITH AN ASTERISK. THE GEOMETRIC DIMENSIONS WERE MEASURED WITH A CALLIPER WITH EXCEPTION FOR THE ELECTRODES.

Parameters	**Top electrode emitter**	**Piezoelectric material emitter**			**Bottom electrode emitter**	**Tungsten plate***			**Bottom electrode receiver**	**Piezoelectric material receiver**			**Top electrode receiver**
	Fitting	***Data***	***Fitting***	***Δ (%)***	***Fitting***	***Data***	***Fitting***	***Δ (%)***	***Fitting***	***Data***	***Fitting***	***Δ (%)***	***Fitting***
t (mm)	0.2	0.5	0.55	9	0.2	3.2	2.9	9.4	0.2	0.6	0.6	0.7	0.02
A (mm²)	177	177	188	6	177	3000	3014	0.7	177	177	186	5	177
ρ (g.cm^{-3})	8.8	7.85	7.85	0	8.8	19.3	19.3	0.01	8.8	7.85	7.85	0	8.8
c_{33} (GPa)	207	121	121	0	207	400	400	0	207	121	121	0	207
Q_m (1)	100	80	80	0	100		300		100	80	80	0	100
h_{33} (×10^9 V.m^{-1})		2.4	2.4	0						2.4	2.4	0	
ε_{33} (F.m^{-1})		823	823	0						823	823	0	
tan δ (%)		1.5	1.5	0						1.5	1.5	0	
tan θ (%)*			1.9								1.9		

in Table 2. Concerning the confidence interval, NOLIAC mentions 5% around the communicated value for mechanical and piezoelectric properties and 10% for electrical ones. As mentioned previously, we focused the fit on the resonances between 2 and 3.5 MHz. We set the voltage generator to 224 mV.

The results provided by Pspice enable an accurate frequency location of the modes for both voltages and powers. Nevertheless, there is a higher global error for the fit with 30% of difference for U_1 and 50% for U_2, this error falls to 20% for both voltages and powers between 2 and 3.5 MHz. This difference can be explained by the resonance at 1.2 MHz and the increase of the voltage at 4 MHz which made the fit difficult. Moreover, the input voltage has an offset which is not due to the piezoelectric emitter as, after study of the electric impedance of this latter, the electrical circuit between the generator and the emitter seems to create this offset.

The parameters are all fit in the confidence intervals provided by the manufacturer. The electrodes are estimated thicker due to the wiring of the transducers. While the STEMINC transducers had their electrodes directly wired on the transducer, the NOLIAC have their negative electrodes wired to the tungsten plate making the glue included in the electrode.

The top electrode of the receiver is also estimated thinner than the bottom electrode of the emitter which can be explained by the variation of the thickness of the weld on the electrode having an impact on the acoustic behavior of the transducer.

Finally, we can observe multiple modes on Fig. 6 which are not simulated by Pspice between 1 and 2 MHz which could be linked to our assumption of couplings modes.

IV. Conclusion

Acoustic Power Transfer has become an important subject of study especially for medical implants applications. This article shows a simplified model of acoustic power transfer of Mason model implemented in Pspice. The simulation provides a qualitative fit enabling to predict the APT for more complex systems made of n-layers integrated in full wireless implant charging structures. However, the simulation has shown its limits and some adjustments need to be done such as the inclusion of the radial modes or the coupling between modes for instance.

Acknowledgment

This work has been accomplished in TIMA laboratory within the scientific environment provided by the Fédération des Micro et NanoTechnologies (FR2542). The authors would also like to thank the CIME Nanotech and especially Gaëtan Debontride who helped in the implementation of the experiment.

References

[1] H. Basaeri, D. B. Christensen, and S. Roundy, “A review of acoustic power transfer for bio-medical implants,” Smart Mater. Struct., vol. 25, no. 12, p. 123001, Nov. 2016.

[2] J. Sperzel et al., “State of the art of leadless pacing,” EP Eur., vol. 17, no. 10, pp. 1508–1513, Oct. 2015.

[3] P. Liu, T. Gao, and Z. Mao, “Analysis of the Mutual Impedance of Coils Immersed in Water,” Magnetochemistry, vol. 7, no. 8, Art. no. 8, Aug. 2021.

[4] U.S. Food and Drug Administration. FDA, "Marketing Clearance of Diagnostic Ultrasound Systems and Transducers". Last accessed: Feb. 27, 2024. https://www.fda.gov/regulatory-information/search-fda-guidance-documents/marketing-clearance-diagnostic-ultrasound-systems-and-transducers

[5] M. Song et al., “Wireless power transfer based on novel physical concepts,” Nat. Electron., vol. 4, no. 10, Art. no. 10, Oct. 2021.

[6] A. Bychkov, V. Simonova, V. Zarubin, E. Cherepetskaya, and A. Karabutov, “The Progress in Photoacoustic and Laser Ultrasonic Tomographic Imaging for Biomedicine and Industry: A Review,” Appl. Sci., vol. 8, no. 10, Art. no. 10, Oct. 2018.

[7] STEMINC, “Piezo Ceramic Disc 20x0.8mm R 2.5 MHz, Manufacturer part number: SMD20T08F2500R”. Last accessed: Feb. 27, 2024. https://www.steminc.com/PZT/piezo-ceramic-disc-20x08mm-r-25-mhz

[8] T. J. Lawry et al., “Electrical optimization of power delivery through thick steel barriers using piezoelectric transducers,” in Energy Harvesting and Storage: Materials, Devices, and Applications, SPIE, Apr. 2010, pp. 216–227.

[9] K. Ono, “A Comprehensive Report on Ultrasonic Attenuation of Engineering Materials, Including Metals, Ceramics, Polymers, Fiber-Reinforced Composites, Wood, and Rocks,” Appl. Sci., vol. 10, p. 2230, Mar. 2020.

[10] W.,P. Mason, "Electromechanical Transducers and Wave Filters", NJ, Princeton, Van Nostrand, 1948.

[11] W. M. Leach, “Controlled-source analogous circuits and SPICE models for piezoelectric transducers,” IEEE Trans. Ultrason. Ferroelectr. Freq. Control, vol. 41, no. 1, pp. 60–66, Jan. 1994.

[12] R. S. Dahiya, M. Valle, and L. Lorenzelli, “SPICE model for lossy piezoelectric polymers,” IEEE Trans. Ultrason. Ferroelectr. Freq. Control, vol. 56, no. 2, pp. 387–395, Feb. 2009.

[13] MatWeb website. Last accessed: Feb. 27, 2024. https://www.matweb.com/

[14] STEMINC, “Piezo Materials Properties” Last accessed: Feb. 27, 2024. http://www.steminc.com/piezo/PZ_property.asp

[15] J.-M. Galliere, P. Papet, and L. Latorre, “A unified electrical SPICE model for piezoelectric transducers,” in 2007 IEEE International Behavioral Modeling and Simulation Workshop, San Jose, CA, USA: IEEE, Sep. 2007, pp. 138–142.

[16] V. T. Rathod, “A Review of Acoustic Impedance Matching Techniques for Piezoelectric Sensors and Transducers,” Sensors, vol. 20, no. 14, p. 4051, Jul. 2020.

[17] NOLIAC “Noliac piezoceramic material NCE51”. Last accessed: Feb. 27, 2024. http://www.noliac.com/products/materials/nce51/